



OPEN

Reduced glucosinolate content in oilseed rape (*Brassica napus* L.) by random mutagenesis of *BnMYB28* and *BnCYP79F1* genes

Srijan Jhingan¹, Hans-Joachim Harloff¹, Amine Abbadi², Claudia Welsch³, Martina Blümel³, Deniz Tasdemir^{3,4} & Christian Jung¹✉

The presence of anti-nutritive compounds like glucosinolates (GSLs) in the rapeseed meal severely restricts its utilization as animal feed. Therefore, reducing the GSL content to <18 $\mu\text{mol/g}$ dry weight in the seeds is a major breeding target. While candidate genes involved in the biosynthesis of GSLs have been described in rapeseed, comprehensive functional analyses are missing. By knocking out the aliphatic GSL biosynthesis genes *BnMYB28* and *BnCYP79F1* encoding an R2R3 MYB transcription factor and a cytochrome P450 enzyme, respectively, we aimed to reduce the seed GSL content in rapeseed. After expression analyses on single paralogs, we used an ethyl methanesulfonate (EMS) treated population of the inbred winter rapeseed 'Express617' to detect functional mutations in the two gene families. Our results provide the first functional analysis by knock-out for the two GSL biosynthesis genes in winter rapeseed. We demonstrate that independent knock-out mutants of the two genes possessed significantly reduced seed aliphatic GSLs, primarily progoitrin. Compared to the wildtype Express617 control plants (36.3 $\mu\text{mol/g}$ DW), progoitrin levels were decreased by 55.3% and 32.4% in functional mutants of *BnMYB28* (16.20 $\mu\text{mol/g}$ DW) and *BnCYP79F1* (24.5 $\mu\text{mol/g}$ DW), respectively. Our study provides a strong basis for breeding rapeseed with improved meal quality in the future.

Oilseed rape or rapeseed (*Brassica napus* L.) is an essential oil crop, ranking as the third-largest source of vegetable oil globally (<http://www.fao.org/faostat/>). In Europe, it is grown as a winter crop, sown in autumn and flowering in the following spring after exposure to cold temperatures over winter. The seeds contain 45–50% oil with a healthy lipid profile, suitable for human consumption¹. Moreover, it is utilized for biodiesel production. After oil extraction, the rapeseed meal (RSM) serves as a protein-rich (40%) animal feed. However, major anti-nutritive compounds like glucosinolates (GSLs) in RSM adversely affect its nutritional and commercial value². Therefore, increasing yield potential, seed oil content, and improving seed meal quality are major goals for rapeseed breeding.

GSLs are diverse heterogeneous secondary metabolites specific to Brassicales. They are sulfur and nitrogen-containing products derived from glucose and amino acids as precursors, comprising a thioglucose and a sulfonated oxime attached to the chain elongated amino acid. Depending on their respective amino acid precursors, GSLs are categorized as aliphatic, aromatic, and indolic, originating primarily from methionine, phenylalanine, and tryptophan, respectively³. Biosynthesis of the three types is independently controlled by distinct gene families⁴. Roughly 130 different GSL types have been described from 16 dicot angiosperms⁵, most of which are edible plants^{6,7}. Apart from *B. napus*, *B. oleracea* (cauliflower, cabbage, broccoli, Brussels sprouts, and kale), and *B. rapa* (turnips and radish) are economically relevant vegetables rich in GSLs^{4,8}. Fifteen major GSL types have been identified in *B. napus*⁶, reaching levels as high as 60–100 $\mu\text{mol/g}$ dry weight in seeds with the methionine-derived aliphatic GSLs constituting up to 92% of all GSL types⁹. The development of rapeseed varieties with low GSL seed content was a milestone in rapeseed breeding¹⁰. Alleles conferring low seed GSL content were introgressed from the Polish spring variety 'Bronowski'¹¹ to develop modern rapeseed cultivars

¹Plant Breeding Institute, Christian-Albrechts-University of Kiel, Am Botanischen Garten 1-9, 24118 Kiel, Germany. ²NPZ Innovation GmbH, Hohenlieth-Hof, 24363 Holtsee, Germany. ³GEOMAR Centre for Marine Biotechnology (GEOMAR-Biotech), Research Unit Marine Natural Product Chemistry, GEOMAR Helmholtz Centre for Ocean Research Kiel, Am Kiel Kanal 44, 24106 Kiel, Germany. ⁴Christian-Albrechts-University of Kiel, Christian-Albrechts-Platz 4, 24118 Kiel, Germany. ✉email: c.jung@plantbreeding.uni-kiel.de

with improved seed meal traits. In modern varieties, the GSL content of the RSM has been reduced to 8–15 μmol per gram seed weight¹⁰.

GSL biosynthesis is completed in three major steps, (i) chain elongation, (ii) core structure formation, and (iii) secondary side-chain modifications³. First, the addition of methylene groups results in chain elongated amino acids. Next, the addition of the sulfur group to the chain-elongated amino acids and S-glucosylation completes the core structure formation. Lastly, secondary modifications like benzoylation, desaturation, hydroxylation, methoxylation, and oxidation result in distinct GSL types^{4,7}. Environmental effects combined with specific genetic mechanisms for GSL biosynthesis, regulation, transport, and storage result in varying GSL contents and diverse profiles observed across *Brassica* species⁷.

GSLs yield toxic by-products after enzymatic cleavage by the endogenous thioglucoside glucohydrolase called myrosinase³. Upon physical injury, the myrosinase is released from so-called ‘myrosin cells’ and comes into contact with GSLs stored in ‘S-cells’¹². Hydrolysis of GSLs generates various products like isothiocyanates (ITC), thiocyanates (SCN), epithionitriles, and nitriles (NI), many of which are known to confer defense against generalist herbivores and bacterial and fungal pathogens¹³. GSLs have been shown to confer antimicrobial properties against the phytopathogenic bacterium *Xanthomonas campestris* pv. *campestris* and the necrotrophic fungus *Sclerotinia sclerotiorum*¹⁴. High consumption of GSLs through the feed can result in several adverse metabolic effects in animals. Hydroxyalkenyl GSLs like epiprogoitrin and progoitrin are goitrogenic by causing inflammation of the thyroid gland⁶. Retarded growth, reduced appetite, and feed efficiency, gastrointestinal irritation, liver and kidney damage, and behavioral effects have been observed in fish¹⁵, poultry¹⁶, and higher mammals like pigs². On the contrary, other GSL types like sulforaphane and indole-3-carbinol are known for their beneficial effects on human health with anti-carcinogenic properties¹⁷.

A complex network of transcription factors (TFs) influenced by abiotic and biotic stimuli, hormonal and epigenetic factors controls the spatiotemporal regulation of GSL biosynthesis^{18,19}. The most notable genes controlling aliphatic GSL biosynthesis in *Arabidopsis* are R2R3 MYB transcription factors. Three TFs *MYB28*, *MYB76*, and *MYB29*, also referred to as *HIGH ALIPHATIC GLUCOSINOLATE (HAG) 1*, *2*, and *3*, respectively, have been described^{18,19}. *HAG1* has been speculated to have a ‘master regulator’ effect by up-regulating almost all genes involved in the core structure formation of aliphatic GSLs¹⁹. In *Brassica* field crops, the role of *MYB28* genes have been demonstrated to be strongly associated with aliphatic GSL biosynthesis in *B. oleracea*²⁰, *B. juncea*^{21–23} and *B. rapa*²⁴. The gene *CYP79F1* controls the first step of the core structure formation by converting chain elongated methionine to corresponding aldoximes^{25,26}. Its role in GSL biosynthesis has also been demonstrated in *B. juncea*²⁷ and *B. oleracea*²⁸.

The transfer of knowledge from *Arabidopsis* to *B. napus* is limited and complicated due to its polyploid genome, where multiple genes with functional redundancies may exist. Several genes associated with GSLs in rapeseed have been revealed through associative transcriptomics, genome-wide association, and QTL mapping studies^{29–33}. These studies demonstrated the significant association between biosynthesis genes *BnMYB28* and *BnCYP79F1* with high aliphatic GSL content.

Our study aimed to reduce aliphatic GSLs in rapeseed since they are the most abundant in seeds. We analyzed the expression profiles of three *BnMYB28* and two *BnCYP79F1* paralogs in rapeseed. Then, we selected *BnMYB28.C09*, *BnMYB28.A03*, *BnCYP79F1.C05* and *BnCYP79F1.A06* as candidate genes for functional studies. Using an ethyl methanesulfonate (EMS) mutagenized winter rapeseed population³⁴, we detected loss-of-function mutations in *BnMYB28* and *BnCYP79F1* genes involved in the core structure biosynthesis of aliphatic GSLs. Double mutants displayed a significant reduction in the seed aliphatic GSL content. These materials could be interesting for breeding rapeseed with improved seed meal quality by achieving a further reduction of aliphatic GSLs in the seeds.

Material and methods

Plant material and growth conditions. We used the oilseed rape EMS population previously developed using an advanced inbred line (F_{11}) of the winter rapeseed variety ‘Express’³⁴. Seeds were treated with 0.5–1.2% EMS for 12 h. The resulting M_2 plants were selfed to produce the corresponding M_3 populations. M_3 plants were grown in 11 cm pots under greenhouse conditions (16 h light, 20–25 °C) for three weeks, with non-mutagenized plants of Express617 as controls. They were vernalized for eight weeks in a cold chamber (16 h light, 4 °C). Plants selected for crossing experiments were hand-pollinated after emasculation. The inflorescences of plants chosen for selfing were isolated with plastic bags before anthesis. Plants selected for GSL measurements were grown in 11 cm pots under greenhouse conditions (16 h light, 20–25 °C).

DNA isolation and PCR. For genomic DNA isolation, leaf samples were collected and lyophilized for 72 h (Martin Christ Gefriertrocknungsanlagen GmbH, Germany). Freeze-dried samples were pulverized using the GenoGrinder2010 (SPEX® SamplePrep LLC, USA) at 1,200 strokes/min. Genomic DNA was isolated using the standard CTAB method³⁵. PCR was performed using paralog-specific primers as per the following conditions: 94 °C for 2 min, 36 cycles of 94 °C for 30 s, 58–66 °C for 30 s–1 min and 72 °C for 1 min, followed by 72 °C for 5 min for final elongation.

Bioinformatics analyses. Genomic DNA and polypeptide sequences of aliphatic GSL biosynthesis genes *AtMYB28* and *AtCYP79F1* were retrieved from The Arabidopsis Information Resource (TAIR—<https://www.arabidopsis.org/>). Using the Darmor-bzh (<http://www.genoscope.cns.fr/brassicnapus/>) and Express617³⁶ rapeseed reference genomes, amino acid sequences of the *Arabidopsis* orthologs were used as BLAST queries. Retrieved chromosomal locations and gene sequences of hits with the lowest e-values and > 80% sequence similarity were accepted. Gene annotations (exons, 5’ and 3’ untranslated regions and open reading frames) for the

paralogs were made using the CLC Main workbench 7 (QIAGEN® Aarhus A/S, Aarhus C, Denmark). Sequence alignments were generated for the genomic DNA, cDNA, and amino acid sequences of the retrieved genes. Conserved and functional domain analyses were done using the NCBI Conserved Domain Database.

Gene expression analysis by RT-qPCR. The winter-type rapeseed inbred line Express617 was used for expression studies. Seeds were sown in 11 cm pots under greenhouse conditions (16 h light, ~25 °C). After three weeks, plants were vernalized (16 h light, 4 °C) for eight weeks and then transferred to greenhouse conditions (16 h light, ~25 °C) and their positions were randomized twice a week. Flowers were hand-pollinated and marked with pollination dates. Leaves and seeds were sampled at 15, 25, 35, and 45 days after pollination (DAP). 50–100 mg of fresh weight tissues were collected from five biological replicates at the four developmental stages. Tissues were frozen in liquid nitrogen and stored at –70 °C. Frozen tissues were pulverized in 2 ml reaction tubes with three 3 mm steel balls using the GenoGrinder2010 (SPEX® SamplePrep LLC, USA) at 1200 strokes/min in 1 min intervals. RNA was isolated using the peqGold Plant RNA Kit (PEQLAB Biotechnologie GmbH, Germany) following the manufacturer's instructions. RNA quality was assessed with a NanoDrop2000 spectrophotometer (ThermoFisher Scientific, USA) and by agarose gel electrophoresis (1.5% agarose, 100 V, 30 min). The RNase-free DNase kit (ThermoFisher Scientific, USA) was used to treat samples with DNaseI to remove contaminating gDNA. cDNA was synthesized with 1 µg RNA using the First Strand cDNA Kit (ThermoFisher Scientific, USA). RT-qPCR was performed on the Bio-Rad CFX96 Real-Time System (Bio-Rad Laboratories GmbH, Germany) using paralog-specific primers (Supplementary Table S1). The relative expression was calculated according to the $\Delta\Delta C_q$ method for each paralog normalized against the two reference genes *BnGAPDH* and *BnACTIN*. The relative expression levels of each candidate paralogs were determined as a mean of five biological replicates with three technical replicates each.

Conventional gel-based detection of EMS induced mutations. We screened 3840 M_2 plants from the EMS-mutagenized winter rapeseed Express617 population³⁴ to detect EMS-induced mutations in *BnMYB28* and *BnCYP79F1* paralogs. Paralog-specific primers were designed for the selected paralogs using the Darmorbzh reference genome (Supplementary Table S2). Amplicons were evaluated for specificity using agarose gel electrophoresis (1% agarose, 100 V, 10 min) and Sanger sequencing for validation. Using the protocol described by Till et al. (2006), we amplified M_2 DNA pools using 5' end infrared labeled probes DY-681 and DY-781 (Biomers, Ulm, Germany) for forward and reverse primers (100 pmol/µl), respectively. The resulting amplicons were processed for heteroduplex formation prior treatment with CELI nuclease (15 min at 45 °C). 5 µl of 50 mM EDTA (pH 8.0) was added to terminate the digestion reaction. After digestion, samples were purified on Sephadex G-50 Fine columns (GE Healthcare, USA). 4 µl of formamide-containing dye (96% deionized formamide, 5 ml 0.25 M EDTA, 0.01% bromophenol blue) was added to each sample. Samples were concentrated to ~20% of the original volume after incubation at 95 °C for 30 min. 0.65 µl concentrated samples were separated on polyacrylamide gels using the LI-COR 4300 DNA Analyzer (LI-COR Biosciences, USA) using standard parameters (1,500 V, 40 mA, and 40 W for 4 h 15 min). The GelBuddy imaging software³⁸ was used to analyze gel images and identify single M_2 mutants. Standard PCR was done to amplify regions harboring the expected single mutations using the gDNA isolated from single M_2 plants. Amplicons were Sanger sequenced to validate the detected EMS-induced point mutations. Mutation effects conferred by SNPs on the polypeptide level were then characterized. Mutation frequencies (F) were estimated following the formula given by Harloff et al. (2012)³⁴:

$$F[1 \text{ per kb}] = 1 / \frac{(\text{amplicon size} - 100) \times \text{number of } M_1 \text{ plants}}{\text{Number of screened mutations} \times 1000}$$

Mutant genotyping. Using standard PCR, primers flanking detected EMS mutations were used for amplification (Supplementary Table S2). PCR specificity was checked using agarose gel electrophoresis (1%, 100 V, 12–30 min). Plants were genotyped by Sanger sequencing of PCR fragments to confirm the presence of EMS mutations.

Glucosinolate measurements. GSLs in leaves and mature seeds were measured in two ways. Quantitative measurements were performed with an enzymatic assay using myrosinase/thioglucoisidase from *Sinapis alba* (Sigma-Aldrich CAS-No. 9025-38-1) and a D-Glucose Assay Kit (glucose oxidase/peroxidase; GOPOD assay) (Megazyme International, Ireland). A qualitative assessment of GSL profiles was done using high-performance liquid chromatography (HPLC). 5–7 g fresh leaves (~15 days after pollination) and 200–600 mg mature seeds were sampled in 50 ml and 2 ml sample tubes, respectively. Sampled leaves were lyophilized for 72 h (Martin Christ Gefriertrocknungsanlagen GmbH, Germany). Freeze-dried leaf samples and mature seeds (BBCH 89) were pulverized using the GenoGrinder2010 (SPEX® SamplePrep LLC, USA) at 1400 strokes/min in 4–5 min intervals. Using the hot methanol (70%) extraction method, ~200 mg milled samples were used to prepare crude extracts following the protocol of Fiebig and Arens (1992)³⁹ and then stored at –20 °C.

For quantitative measurements, crude extracts (4 ml) were passed through 0.5 ml DEAE-Sephadex A-25 columns (GE Healthcare, USA). The bound GSL was digested on the column for 18 h at room temperature with ~0.8 U myrosinase/thioglucoisidase. After digestion, columns were washed twice with 0.5 ml deionized distilled water (ddH₂O) for elution of glucose. The eluate was shock frozen and freeze-dried for ~72 h. The residue was dissolved in 100 µl ddH₂O and a 5–40 µl aliquot was used for analysis in duplicates using the D-Glucose Assay Kit (Megazyme International, Ireland) following the manufacturer's instructions.

For qualitative analyses, GSL in 1 ml crude extracts were bound on 250 µl DEAE-Sephadex A-25 columns and digested on the column for 18 h at room temperature with 18 U sulfatase H1 enzyme (Merck KGaA, Germany). Desulfoglucosinolates were eluted twice with 1 ml ddH₂O. 10–50 µl aliquots were separated on a 250 × 4.6 mm Lichrosorb 5µ column (Merck KGaA, Germany) as described by Fiebig and Arens (1992)³⁹ using a Shimadzu2000 HPLC-system. GSLs were quantified by their absorbance at 229 nm and identified by retention time using commercially available GSL standards (PhytoLab GmbH, Germany). For each commercially available standard, an individual calibration curve was used for quantification (Supplementary Table S3).

To validate peak identity and quantification, a test set of 8 seed extract samples (concentration 8 mg/ml) from HPLC measurements were analyzed for cross-referencing on an LC–MS system consisting of a VWR Hitachi Elite LaChrom (Hitachi High-Technologies Corporation, Japan), L-2450 DAD detector, L-2300 Column Oven, L-2200 Autosampler and L-2130 Pump connected to an iontrap esquire4000 (Bruker Daltonics, Germany). The chromatography was carried out on a Synergi 4 µ Polar-RP column (80 Å, 250 × 4.6 mm, Phenomenex, Torrance, USA). The mobile phase consisted of H₂O (Milli-Q grade, Arium® Water Purification Systems, Sartorius, Germany) with 0.1% formic acid (Promochem, ScienTest-BioKEMIX GmbH, Germany) as eluent A, and acetonitrile (LC–MS-grade, AppliChem, Germany) as eluent B⁴⁰. The following chromatographic conditions were applied: elution starting from 0% B 0–2 min isocratic, gradient elution from 2 to 12 min to 60% B, 12–14 min isocratic elution at 60% B, gradient elution from 14 to 15 min to 0% B, 15–23 min isocratic re-equilibration at 0% B, 1 ml/min flow, oven temperature 30 °C, wavelength 229 nm, injection volume 50 µl. The iontrap settings were as follows: negative mode, capillary voltage: 4000 V, nebulizer: 50 psi, dry gas (nitrogen): 10.0 L/min, dry temperature: 365 °C, scan range: 100–1200 m/z⁴⁰.

Major sample peaks were quantified at 229 nm using a VWR Hitachi Chromaster (Hitachi High-Technologies Corporation, Japan) consisting of a 5430 DAD detector, 5310 Column Oven, 5260 Autosampler, and a 5110 Pump. The chromatographic conditions were applied as described for the LC–MS system, except that no formic acid was added to eluent A. The injection volume was 30 µl.

Statistical analyses. For expression studies, significantly expressed paralogs were identified by performing an ANOVA ($p < 0.05$) for the relative expression levels of each paralog. Mean relative expressions from five biological replicates were compared across the four sampling points 15, 25, 35, and 45 DAP in seeds and leaves. The LSD test ($\alpha \leq 0.05$) was performed to generate statistical groups using the ‘Agricolae’ package in R. The standard error of the mean was calculated across the five biological replicates with three technical replicates each.

In GSL determination experiments, the total GSL content using the D-Glucose Assay Kit and the contents of individual GSL compounds using HPLC were evaluated for statistical significance across the analyzed samples. An ANOVA ($p < 0.05$) was performed for the analysis of the variance along with an LSD test ($\alpha \leq 0.05$) for statistical grouping using the ‘Agricolae’ package in R. The standard error of the mean was calculated across five biological replicates.

Results

Identification of MYB28 and CYP79F1 genes in the oilseed rape genome. For identification of possible paralogs in rapeseed, the Darmor-*bzh* reference genome (<https://www.genoscope.cns.fr/brassiccanapus/>) was searched for MYB28 and CYP79F1 genes using polypeptide sequences from *A. thaliana* genes *AtMYB28* (AT5G61420) and *AtCYP79F1* (AT1G16410) as queries. Based on the lowest e-values and highest sequence similarities (> 80%), three and two paralogs were detected for *BnMYB28* and *BnCYP79F1*, respectively (Table 1, Supplementary Fig. S1). The polypeptides of *BnMYB28* and *BnCYP79F1* shared a similarity of 85% and 86%, respectively with their corresponding *Arabidopsis* orthologs. We aligned the polypeptide sequences of the candidate paralogs to identify conserved functional domains characteristic for the R2R3 MYB transcription factor and cytochrome P450 gene families (Supplementary Fig. S2). In line with previous reports, the highly conserved DNA binding R2 and R3 domains specific to the subgroup 12 MYB transcription factors and the nuclear localization signal with the ‘LKKRL’ amino acid residues were present across protein sequences of all three *BnMYB28* paralogs⁴¹. The paralog *BnMYB28.C09* was annotated in a truncated form in the Darmor-*bzh*

<i>Arabidopsis</i> gene ¹	<i>B. napus</i> paralogs ^a	<i>B. napus</i> gene name	Chromosomal Location	Gene length (bp)	Coding region (bp)	Polypeptide length	Shared protein identity with the <i>Arabidopsis</i> ortholog (%)
<i>AtMYB28</i>	<i>BnaA03g040190D</i>	<i>BnMYB28.A03</i>	A03	2018	987	328	85.2
	<i>BnaCnnng43220D</i>	<i>BnMYB28.Cnn</i>	Cnn ^b	2072	1011	337	87.1
	<i>BnaC09g05300D</i>	<i>BnMYB28.C09</i>	C09	1072	420	140	82.8
<i>AtCYP79F1</i>	<i>BnaC05g12520D</i>	<i>BnCYP79F1.C05</i>	C05	2397	1623	540	86.1
	<i>BnaA06g11010D</i>	<i>BnCYP79F1.A06</i>	A06	2380	1623	540	85.8

Table 1. Features of *BnMYB28* and *BnCYP79F1* paralogs with homology to the *Arabidopsis* genes *AtMYB28* (AT5G61420) and *AtCYP79F1* (AT1G16410) in oilseed rape. ¹*A. thaliana* gene sequences were retrieved from The Arabidopsis Information Resource (TAIR). ^aSequence analysis of orthologs and paralogs in oilseed rape are based on gene models described in the Darmor-*bzh* reference genome (Genoscope). ^bNot anchored to a specific *B. napus* chromosome.

and Express617 reference genomes but harbored all conserved domains required for gene activity. The protein sequences of both *BnCYP79F1* paralogs possessed five conserved domains characteristic to the family of cytochrome P450 enzymes, including a 'heme' group speculated to act as the catalytic domain²⁵.

Expression profiles of *BnMYB28* and *BnCYP79F1* genes reveal putative functional paralogs. For knock-out studies, we aimed to select highly expressed paralogs. Therefore, we investigated the expression profiles of *BnMYB28* and *BnCYP79F1* genes in the German winter-type inbred rapeseed Express617 by RT-qPCR. The relative expression of candidate genes was analyzed in leaves and seeds at growth stages 15, 25, 35, and 45 days after pollination (DAP).

The two *BnMYB28* paralogs *BnMYB28.C09* and *BnMYB28.A03* showed a thousand fold higher relative expression in leaves than seeds across all growth stages (Fig. 1). *BnMYB28.C09* was the most highly expressed paralog in leaves. However, expression sharply declined 15 DAP and remained low during later stages of seed development (25–45 DAP). The expression of *BnMYB28.A03* was consistently lower across all growth stages in the leaves, accounting for ~ 17% of the expression levels of *BnMYB28.C09*. In leaves *BnMYB28.Cnn* expression was not detectable, whereas measurable expression was detected at later stages towards seed maturity. Conclusively, *BnMYB28.C09* and *BnMYB28.A03* were selected for further studies as putative functional paralogs because they were significantly expressed in the leaves.

Similar to *BnMYB28*, *BnCYP79F1* paralogs were significantly more expressed in the leaves than seeds, attaining a 100-fold higher expression level. There was also a significant difference between the two *BnCYP79F1* paralogs in leaves as the expression of *BnCYP79F1.C05* was more than tenfold higher than *BnCYP79F1.A06* (Fig. 1). In contrast, the expression levels of *BnCYP79F1.A06* was higher than *BnCYP79F1.C05* in seeds. In the early stages of seed development (15 DAP), *BnCYP79F1.A06* was tenfold higher expressed than *BnCYP79F1.C05*, followed by a drastic decrease as the plants matured. In leaves, the expression of *BnCYP79F1.C05* sharply increased between 25 and 35 DAP and then decreased as the plants approached maturity. Interestingly, *BnMYB28* and *BnCYP79F1* genes displayed opposite expression patterns in the leaves. While *BnMYB28* was highly expressed at early stages (15 DAP) followed by a sharp decline, *BnCYP79F1* expression increased during later stages (25–35 DAP).

EMS-induced mutants for selected *BnMYB28* and *BnCYP79F1* paralogs. We screened the M₂ population for EMS-induced mutations in four genes (*BnMYB28.C09*, *BnMYB28.A03*, *BnCYP79F1.C05*, and *BnCYP79F1.A06*) using a conventional polyacrylamide gel-based assay. We detected 35 and 43 EMS-induced mutations in *BnMYB28* and *BnCYP79F1* paralogs, respectively (Supplementary Table S4), which could be classified into 6 nonsense, 50 missense, and 22 silent mutations (Fig. 2). No splice site mutations were detected. Mutation frequencies ranged between 1/31.5 and 1/67.0 kb across the two gene families. On average, a frequency of one EMS-induced mutation per 43.6 kb was detected (Supplementary Table S5), which is in the range of estimations made by former studies on this EMS population^{42–47}. Both *BnMYB28* nonsense mutations were located within the conserved DNA binding R2 domain. Additionally, seven missense mutations were also detected within the R2 domain. We found one nonsense mutation in the *BnCYP79F1.C05* paralog, while none could be detected for *BnCYP79F1.A06*. A missense mutation conferring a minor change to the protein folding due to the exchange of lysine with glutamic acid was selected. For further studies, we chose all M₃ plants with nonsense mutations plus the *BnCYP79F1.A06* missense mutant. For ease of understanding, we assigned unique one-letter codes to wildtype and mutant alleles (Table 2).

Due to high functional redundancies of genes in the polyploid oilseed rape genome, single mutations rarely have a phenotypic effect. Therefore, we crossed single mutants of *BnMYB28.C09* and *BnMYB28.A03* and then separately for *BnCYP79F1.C05* and *BnCYP79F1.A06* to produce distinct double mutants of *BnMYB28* and *BnCYP79F1*, respectively. We genotyped M₃ plants by generating PCR fragments encompassing the expected mutations (Supplementary Table S2) and confirmed single M₃ mutants by Sanger sequencing of the PCR fragments (Supplementary Table S6). Mutant plants were selected for crossing experiments (Supplementary Table S7). *BnMYB28* and *BnCYP79F1* M₃ single mutants were crossed with each other (referred to as 'M₃xM₃'). F₁ offspring were selfed to generate the F₂ populations 200527 (Supplementary Fig. S3A) and 200529 (Supplementary Fig. S3B), respectively.

Mutations in *BnMYB28* and *BnCYP79F1* confer a significant reduction in the aliphatic GSL content in seeds. We investigated the effect of EMS-induced mutations in *BnMYB28* and *BnCYP79F1* genes by quantitative and qualitative analysis of GSLs. Segregating individuals from two F₂ populations (200527 and 200529) were analyzed (Supplementary Table S7) along with non-mutagenized Express617 plants as controls. F₂ populations 200527 and 200529 originated from M₃xM₃ crosses of *BnMYB28* and *BnCYP79F1* single mutants, respectively.

First, F₂ plants from the two populations were genotyped by Sanger sequencing. Four genotypes per population were selected for phenotypic studies. In F₂ populations 200527 and 200529, plants homozygous for the wildtype alleles (*A_eA_eB_eB_e* and *C_eC_eD_eD_e*), homozygous for one mutant allele (*A₁A₁B_eB_e* or *A_eA_eB₁B₁* and *C₁C₁D_eD_e* or *C_eC_eD₁D₁*), and homozygous for two mutant alleles (*A₁A₁B₁B₁* and *C₁C₁D₁D₁*) were selected for phenotyping (Supplementary Fig. S3A,B).

In general, a significantly higher GSL content was observed in seeds than in leaves (Fig. 3). In seeds of *BnMYB28* double mutants (F₂ population 200527), the GSL content was significantly ($p < 0.05$) reduced to 23.41 μmol/g DW compared to F₂ plants homozygous for the wildtype alleles (47.28 μmol/g DW) and the non-mutagenized Express617 control plants (49.73 μmol/g DW), which corresponds to a significant GSL reduction by 50.5% and 52.9%, respectively (Fig. 3). Interestingly, single mutants of *BnMYB28.A03* (26.96 μmol/g DW) showed a significant reduction in seed GSL content in contrast to *BnMYB28.C09* single mutants (49.42 μmol/g

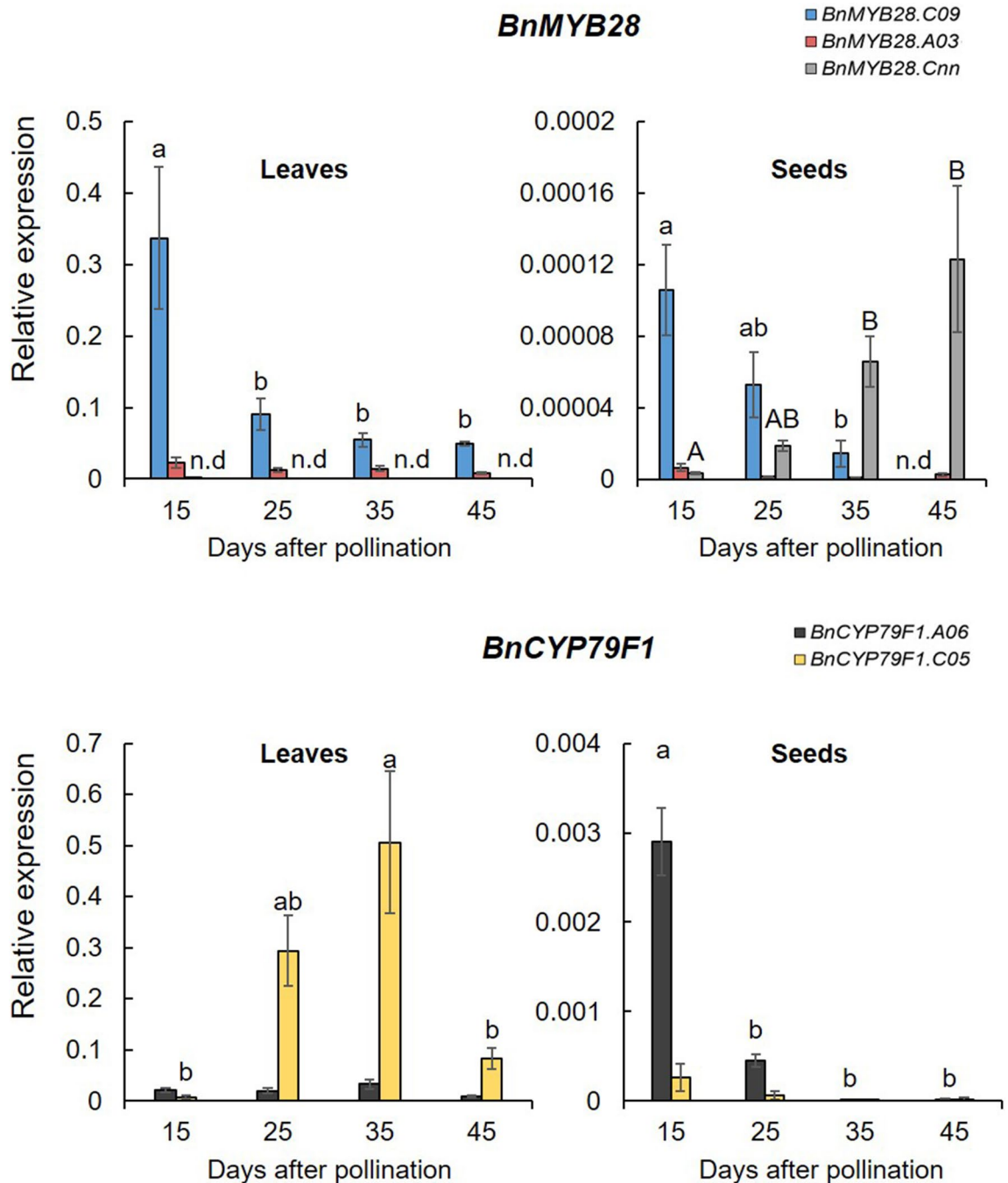


Figure 1. Relative expression of three *BnMYB28* and two *BnCYP79F1* paralogs in the winter-type oilseed rape Express617. Plants were grown in the greenhouse (20–25 °C and 16 h light) after vernalization (4 °C, 16 h light for 8 weeks). For each gene, leaves and seeds were sampled from five plants 15, 25, 35, and 45 days after pollination (five biological replicates). RT-qPCR was performed with three independent samples of each plant (three technical replicates) and the relative expression was calculated after normalization with two reference genes, *BnACTIN* and *BnGAPDH*. Error bars represent the standard error of the mean of five biological replicates, with three technical replicates each. Statistical significance was calculated with an ANOVA ($p < 0.05$, linear model, grouping: Tukey test) using the R package ‘Agricolae’. Alphabets over bars represent statistical groups. n.d: not detectable.

DW). The seed GSL content in *BnMYB28.A03* single mutants were in the range of the *BnMYB28* double mutants. No significant differences were observed between the leaves of *BnMYB28* double mutants (0.96 $\mu\text{mol/g DW}$) and the Express617 control (0.86 $\mu\text{mol/g DW}$). Also, the *BnCYP79F1* double mutants (F_2 population 200529) showed reduced seed GSL contents by 27.9% and 26.9% compared to the Express617 controls and the F_2 plants homozygous for the wildtype alleles, respectively. However, the difference was not statistically significant ($p < 0.05$). GSL

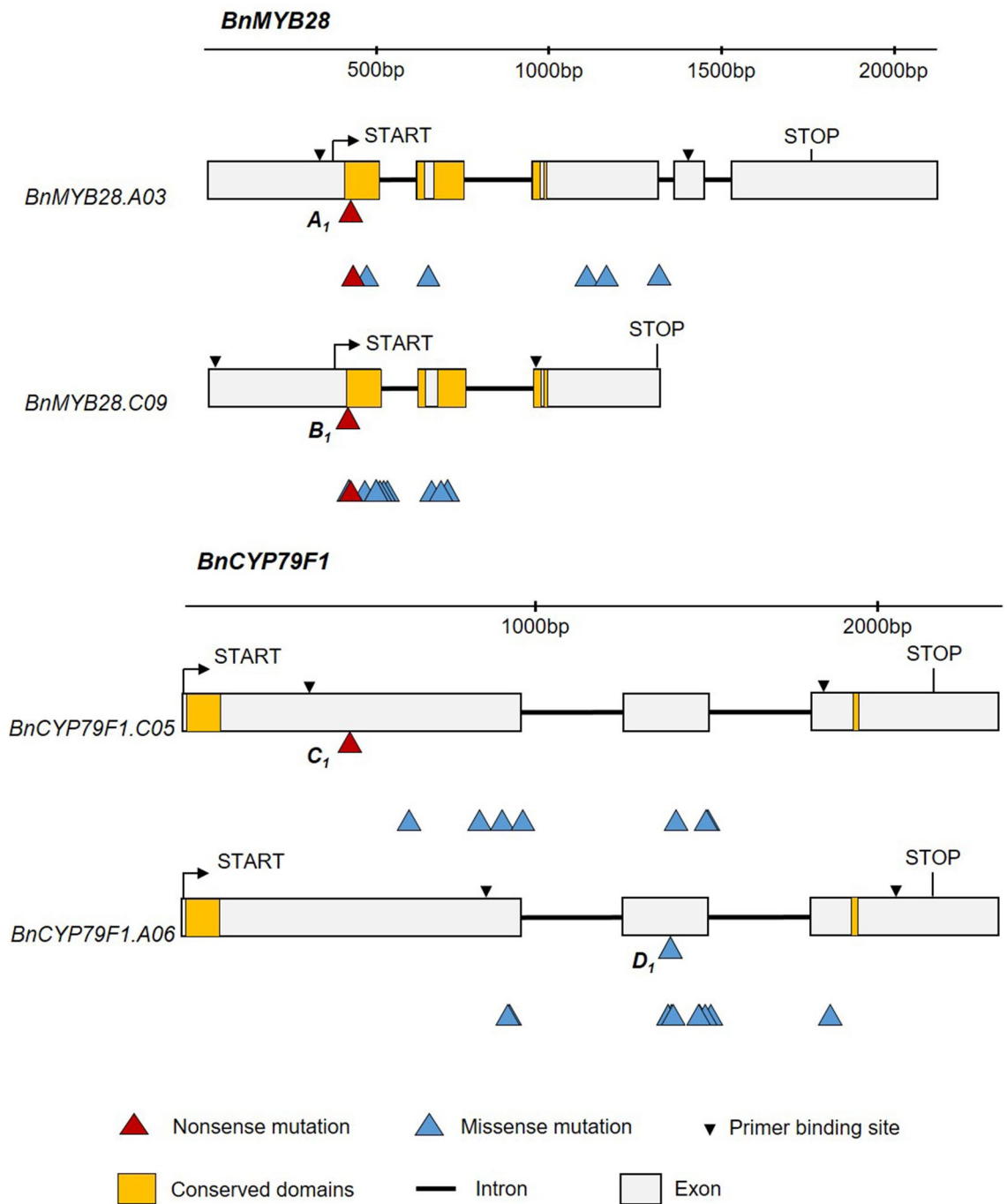


Figure 2. Structure of four *BnMYB28* and *BnCYP79F1* genes and positions of EMS-induced nonsense and missense mutations. Allele identities are given next to the mutation site for those mutations used for further studies (refer to Table 2 for all allele codes). Regions coding for functional and conserved domains characteristic to the gene families are marked in orange boxes. START and STOP represent the translation start and stop sites, respectively. For *BnCYP79F1*, the 5' untranslated regions are not defined on the Darmor-*bzh* reference genome.

contents in leaves varied between 0.9 and 1.5 $\mu\text{mol/g}$ DW in the *BnCYP79F1* double mutants and 0.7–1.5 $\mu\text{mol/g}$ DW in the wildtype F_2 plants without statistically significant differences between the genotypes.

Then, individual seed GSL profiles were analyzed in the same plants as performed for total GSL determination. Single GSLs were identified by retention time and co-chromatography with commercial standards and quantified using individual calibration curves (Supplementary Table S3). Although the estimation of total GSL by summing up the major compounds identified by HPLC yielded generally higher values than the enzymatic method, the results did not show significant differences between mutants (Supplementary Fig. S4). This suggested that our data evaluation for single GSL identification via HPLC and the sum of their concentrations were in line with the total GSL content estimated with the enzymatic test. Eight seed sample extracts were analyzed

	Gene name	Mutation position on gDNA ¹	Allele code	cDNA change ¹	AA change	Mutation type	M ₃ seed code ²
M ₃ single mutants	<i>BnMYB28.C09</i>	G51A	A ₁	G51A	W17*	Nonsense	190623
	<i>BnMYB28.A03</i>	G50A	B ₁	G50A	W17*	Nonsense	190625
	<i>BnCYP79F1.C05</i>	C424T	C ₁	C424T	E142*	Nonsense	190628
	<i>BnCYP79F1.A06</i>	G1379A	D ₁	G1090A	E364K	Missense	190630
Wildtype Express617	<i>BnMYB28.C09</i>	n.a	A _e	n.a			
	<i>BnMYB28.A03</i>		B _e				
	<i>BnCYP79F1.C05</i>		C _e				
	<i>BnCYP79F1.A06</i>		D _e				

Table 2. Allele codes assigned to EMS mutants and wildtype plants selected as crossing parents in this study. Single mutants were selected as crossing parents to combine single mutations for enhanced phenotypic effects. For each of the analyzed paralogs, mutants and wildtype parents were assigned unique allele codes. ¹Position relative to the translation start site. ²M₃ seed codes corresponding to screened M₂ mutants. Non-mutated wildtype alleles from Express617 are represented with the ‘e’ suffix in subscript. *Premature stop codon, n.a not applicable.

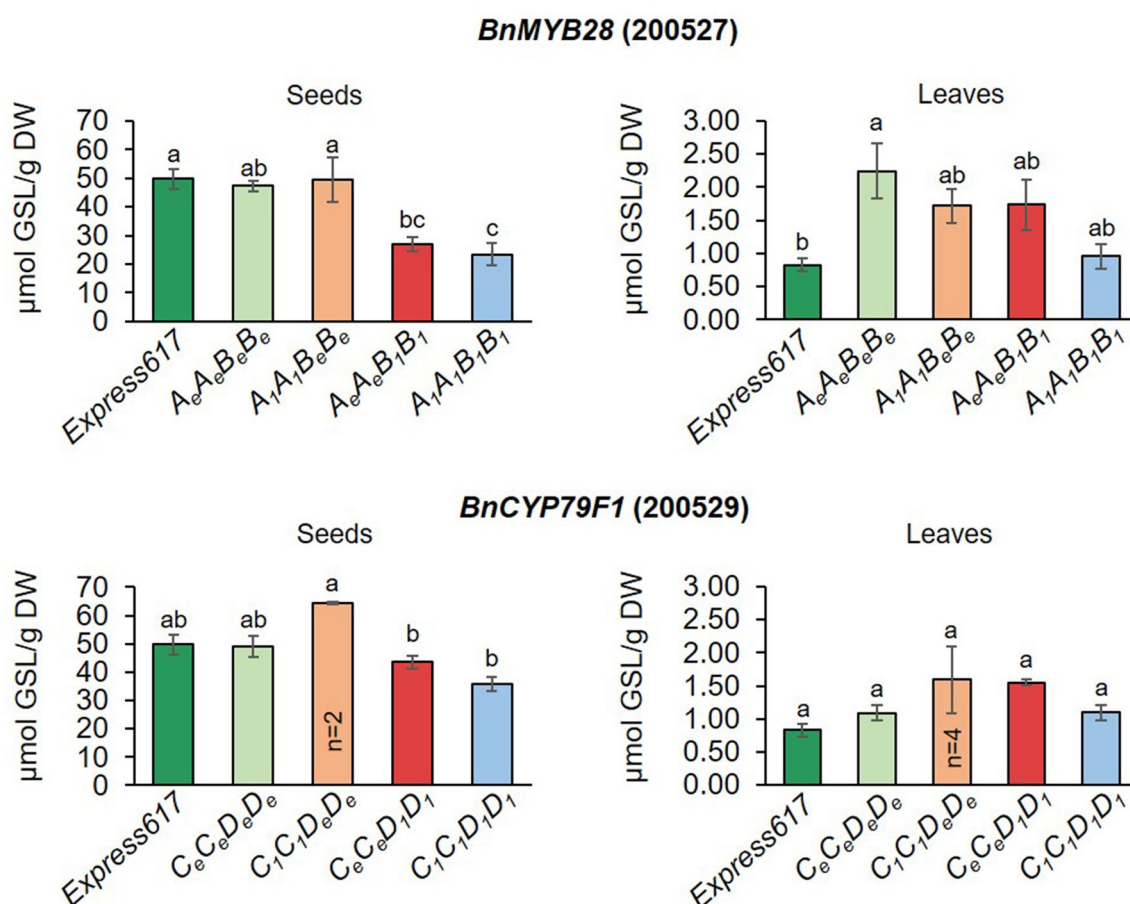


Figure 3. Seed and leaf glucosinolate contents in populations segregating for *BnMYB28* and *BnCYP79F1* mutations. F₂ populations 200527 and 200529 segregating for *BnMYB28* and *BnCYP79F1* mutations, respectively, originated from M₃ × M₃ crosses. Homozygous F₂ double mutants (A₁A₁B₁B₁ and C₁C₁D₁D₁) were analyzed together with homozygous single mutants (A₁A₁B_eB_e, A_eA_eB₁B₁, C₁C₁D_eD_e and C_eC_eD₁D₁), non-mutagenized Express617 and F₂ plants homozygous for the wildtype alleles (A_eA_eB_eB_e and C_eC_eD_eD_e). Leaf samples were taken 15 days after pollination and mature seeds (BBCH89) were used for glucosinolate determination. Error bars represent the standard error from five plants (n = 5) per genotype with two exceptions mentioned in the figure. An ANOVA (*p* < 0.05) was performed and the Tukey test (*p* < 0.05) was done for grouping. Different alphabets above error bars represent groups based on significance. All genotypes are as per designated allele codes given in Table 2.

by LC–MS (Iontrap) to confirm the peak identity. All previously calibrated glucosinolates were confirmed. Moreover, two additional aliphatic glucosinolates (gluconapoleiferin and glucoalyssin) and the major indolic glucosinolate 4-hydroxyglucobrassicin, for which no calibration standards were available, could be identified and were quantified based on their UV absorbance at 229 nm using sinigrin (as internal standard) and calibration factors from the literature³⁹.

In the seeds, we identified nine aliphatic GSLs (glucoiberin, progoitrin, epiprogoitrin, sinigrin, glucoraphanin, gluconapoleiferin, glucoalyssin, gluconapin, and glucobrassicinapin) in varying quantities and four other GSLs (4-hydroxyglucobrassicin, glucotropaeolin, glucobrassicin, and gluconasturtiin) in smaller amounts. In line with previous reports⁹, the aliphatic GSL comprised the major portion (93.9%) of the seed GSL content in all genotypes studied here (Fig. 4).

In *BnMYB28* F₂ double mutants (population 200527), the progoitrin concentrations in seeds were 55.3% lower than in the Express617 controls (reduced from 36.32 $\mu\text{mol/g DW}$ to 16.20 $\mu\text{mol/g DW}$) (Fig. 5, Supplementary Table S8). The next abundant aliphatic compounds in the seeds were gluconapin and glucobrassicinapin. While glucobrassicinapin levels were drastically reduced by 87% from 5.26 $\mu\text{mol/g DW}$ in the Express617 controls to 0.64 $\mu\text{mol/g DW}$ in the double mutants, the gluconapin content was not significantly reduced. The minor aliphatic compound epiprogoitrin, whose synthesis starts from gluconapin, was reduced by 51% (0.57 $\mu\text{mol/g DW}$) in the double mutants compared to Express617 (1.17 $\mu\text{mol/g DW}$). The remaining seed GSLs analyzed did not exceed 3 $\mu\text{mol/g DW}$. Out of the 28 $\mu\text{mol/g DW}$ reduction observed in the total seed GSL content of double mutants, the three major aliphatic GSLs accounted for 86% (24 $\mu\text{mol/g DW}$) of the total reduction. In the *BnCYP79F1* F₂ double mutants, the progoitrin content was 32.4% lower than in Express617 (36.32 $\mu\text{mol/g DW}$ compared to 24.5 $\mu\text{mol/g DW}$) (Fig. 5, Supplementary Table S9). The glucobrassicinapin content was not altered in the *BnCYP79F1* double mutants. However, a 30.4% decrease in gluconapin content suggests that the *BnCYP79F1* mutations might have a bigger effect on the synthesis of short-chained 4C aliphatic than on the 5C aliphatic GSLs.

Discussion

Major anti-nutritive compounds like GSLs in the RSM pose a challenge for utilization as animal feed. Therefore, a major breeding goal is a reduction of the seed glucosinolate content (SGC) to an acceptable limit of < 18 $\mu\text{mol/g}$ dry weight. This study aimed to reduce the aliphatic GSL content in seeds by knocking out *BnMYB28* and *BnCYP79F1* genes involved in the biosynthesis of aliphatic GSLs in rapeseed. We demonstrate that independent knock-out mutants of the two genes possessed significantly reduced total and aliphatic GSLs, primarily progoitrin, in the seeds.

We targeted the aliphatic GSL biosynthesis pathway since the aliphatic profile comprises up to 92% of all GSLs reported from rapeseed⁹. Moreover, major GSLs such as progoitrin that have adverse metabolic effects in animals belong to the aliphatic profile^{6,16,48}. We reasoned that functional mutations in genes involved in the

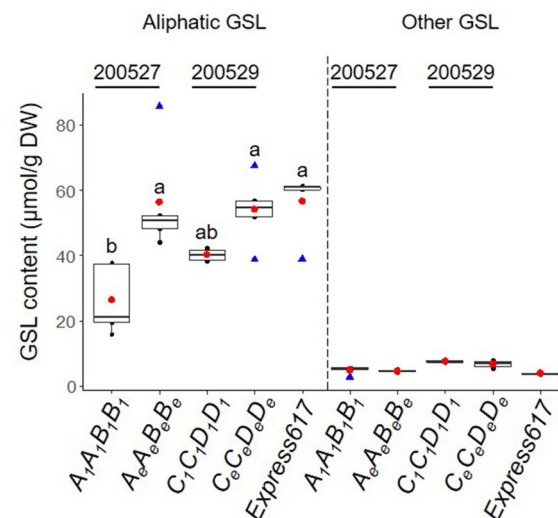


Figure 4. Analysis of major glucosinolate types in mature seeds of *BnMYB28* and *BnCYP79F1* mutants. Aliphatic and other GSL types measured from homozygous *BnMYB28* (genotype A₁A₁B₁B₁, seed code 200527) and *BnCYP79F1* (genotype C₁C₁D₁D₁, seed code 200529) originating from M₃xM₃ crosses. F₂ plants homozygous for the wildtype alleles (A_eA_eB_eB_e and C_eC_eD_eD_e) and non-mutated Express617 were used as controls. Plants were grown in the greenhouse. Mature seeds were harvested at BBCH89. GSL profiles for aliphatic and other GSL types (phenolic and indolic) were analyzed using HPLC. GSL content was calculated as $\mu\text{mol/g}$ dry weight (DW). Individual and mean values are marked in black and red dots, respectively. Blue triangles represent outliers. Error bars represent the standard error of the mean from five biological replicates. An ANOVA test ($p < 0.05$) was performed and significant differences between groups were calculated by a Tukey test ($p < 0.05$). Different alphabets above error bars represent groups based on significance. All genotypes are as per designated allele codes given in Table 2.

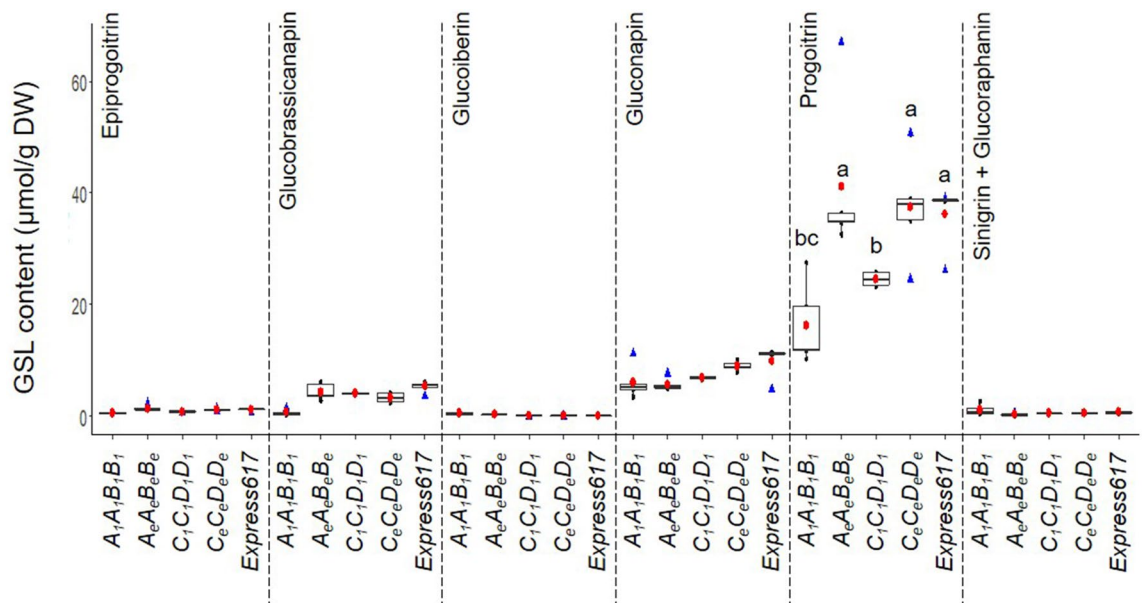


Figure 5. Analysis of aliphatic glucosinolates in mature seeds of *BnMYB28* and *BnCYP79F1* mutants. Individual aliphatic GSLs in homozygous F_2 *BnMYB28* (genotype $A_1A_1B_1B_1$, seed code 200527) and *BnCYP79F1* (genotype $C_1C_1D_1D_1$, seed code 200529) double mutants originating from $M_3 \times M_3$ crosses. F_2 plants homozygous for the wildtype alleles ($A_eA_eB_eB_e$ and $C_eC_eD_eD_e$) and non-mutated Express617 were used as controls. Aliphatic GSLs were identified and quantified using HPLC. The content was calculated as $\mu\text{mol/g}$ dry weight (DW). Individual values and mean values are marked in black and red dots, respectively. Blue triangles represent outliers. Error bars represent the standard error of the mean from biological replicates. An ANOVA test ($p < 0.05$) was performed and significant differences between groups were calculated by a Tukey test ($p < 0.05$). Different alphabets above error bars represent groups based on significance. All genotypes are as per designated allele codes given in Table 2. *n.d.* not detectable.

secondary modification of GSLs might only confer an altered GSL profile and not a significant reduction in the overall content. Therefore, we selected *BnMYB28* and *BnCYP79F1* due to their prominent role in the core structure formation of aliphatic GSLs^{18,25}. In *Arabidopsis*, a transcriptome study confirmed the role of sub-group 12 R2R3 MYB transcription factors in up-regulating almost all genes involved in the core structure formation of aliphatic GSLs¹⁹. In associative transcriptomics and QTL mapping studies, former studies have found *MYB28* and *CYP79F1* to be strongly associated with a high aliphatic GSL content in rapeseed^{49,50}. More recently, Kittipol et al. (2019)³⁰ and Liu et al. (2020)³³ have also identified *MYB28* as a significant gene controlling aliphatic GSL content in rapeseed using transcriptome and genome-wide association studies, respectively.

It has been demonstrated that the biosynthesis of GSLs occurs in vegetative parts, especially in rosette leaves and silique walls⁵¹. Using histochemical analyses in *Arabidopsis*, Reintanz et al. (2001)²⁵ have demonstrated that the activity of the biosynthesis gene *CYP79F1* is restricted to the silique walls, and almost untraceable expression levels were observed in the seeds. Moreover, in silico microarray analyses have shown that the expression of the *CYP79F1* and the *MYB28* transcription factors in *Arabidopsis* seeds was insignificant⁵². The negligible expression levels of genes involved in the chain elongation and GSL core-structure formation steps in seeds strongly suggest their inability for the de novo synthesis of GSLs⁵². Our expression analyses for *BnMYB28* and *BnCYP79F1* paralogs encompass seed setting and loading phases between 15 and 45 days after pollination (DAP). In our study, the expression profiles observed for the two biosynthesis genes complement previous studies since expression levels were significantly higher in leaves than seeds. *BnMYB28* paralogs were expressed thousand fold higher in the leaves. Relative expression levels increased during the early growth stages (15 DAP) with a gradual decrease as the plant approached maturity (45 DAP). This was expected since GSL biosynthesis increases as the plant transitions from the vegetative to the generative phase^{18,53}. In *Arabidopsis*, Brown et al. (2003)⁵³ have demonstrated that towards maturity, the reduction in leaf GSL content is concurrent with an increasing GSL content in the seeds. *BnMYB28.C09* showed the most significant expression levels over other gene copies in the leaves. In previous mapping studies, QTL significantly associated with high aliphatic GSL content in leaves and seeds of rapeseed were linked to *BnMYB28* on chromosome C09^{29,50,54,55}. Although *BnMYB28.Cnn* showed higher relative expression than other paralogs in seeds towards maturity, its levels were in trace amounts. Moreover, its expression in leaves was undetectable. Since GSL biosynthesis is absent in seeds, we reason that the expression levels of *BnMYB28.Cnn* are too low to affect the seed GSL content. Most genes involved in aliphatic GSL biosynthesis, including *CYP79F1*, are under the transcriptional control of *MYB28*¹⁹. This was evident since a significantly high relative expression of *BnMYB28.C09* at 15 DAP was followed by a significant increase in *BnCYP79F1.C05* expression levels in the leaves at 25 DAP. Based on these data, we reasoned paralogs *BnMYB28.C09* and *BnCYP79F1.C05* as our most promising candidates for functional analyses due to their significant expression levels in leaves, the primary site for GSL biosynthesis. However, due to the high functional redundancy in the polyploid rapeseed genome, we cannot wholly rely on single mutants of highly expressed paralogs for significant

phenotypic effects. Therefore, we also considered *BnMYB28.A03* and *BnCYP79F1.A06* for pyramiding functional mutants for enhanced phenotypic effects.

Former studies demonstrating EMS-induced random mutagenesis in Brassicaceae crops have reported a wide range of mutation frequencies between 1/12 and 1/447 kb^{34,56–60}. In this work, we screened the EMS-mutagenized population of the winter rapeseed ‘Express617’ developed by Harloff et al. (2012)³⁴. Past studies on this resource have estimated varying mutation frequencies of 1/24–1/72 kb^{42–47}. This variation is expected since frequency estimations depend on factors like the length of amplicons screened, the GC content within amplified fragments, and the number of pools screened for mutant detection. We estimated an average mutation frequency of 1/52.4 kb for *BnMYB28* and 1/34.7 kb for *BnCYP79F1*, which is well within the frequencies expected from this mutant population.

The functionality of R2R3 MYB transcription factors is determined by the DNA binding R2 and R3 domains and a nuclear localization signal^{18,61}. We detected EMS-induced nonsense mutations within the conserved R2 domain in the first exons of *BnMYB28.C09* and *BnMYB28.A03*. Since both premature nonsense mutations were located in the R2 conserved domain, consequent transcripts are expected to lack the downstream R3 DNA binding and the vital NLS domains. For both single mutants, >95% of the resultant protein sequence is expected to be truncated. Therefore, we anticipate a complete loss-of-function of the *BnMYB28* transcription factor in selected mutants.

Within *BnCYP79F1.A06*, only missense mutations were found. A lack of nonsense mutations could be due to two reasons. First, the paralog-specific primers encompassed only 38% of the total cDNA sequence. Second, the amplicon possessed only five possible amino acid motifs with the possibility of converting to stop codons after the EMS-induced C → T or G → A transitions. Since we observed a nearly undetectable gene expression for *BnCYP79F1.A06* in the leaves compared to *BnCYP79F1.C05*, we speculate that its role in the biosynthesis process is less critical. Moreover, associative transcriptomics studies have reported *BnCYP79F1.C05* to be significantly correlated with the aliphatic GSL content in rapeseed³⁰.

Based on functional studies from *Arabidopsis*^{18,25} and *Brassica* crops^{21,22,24,27,28}, we expected that a knock-out of the two genes would severely influence the biosynthesis of short-chained aliphatic GSLs, especially progointrin that accounts for ~80% of all GSLs in the seeds³. Since progointrin is also the most abundant seed GSL type in rapeseed⁹, we anticipated significant changes in the mutants. In this regard, a more significant effect from *BnMYB28* mutants was expected due to its central regulatory control over the aliphatic GSL biosynthesis^{18,19}. Therefore, a knock-out of the *BnMYB28* is expected to downregulate several genes involved in the biosynthesis process. We reasoned that a knock-out of the *BnMYB28* transcription factor alone would have a significant effect on seed GSL levels and a *BnMYB28/BnCYP79F1* double mutant was not expected to display an enhanced phenotypic effect. For validation, we suggest analyzing the expression of major downstream targets in *BnMYB28* double mutants, e.g., *MAM3*⁶², which is involved in chain elongation and *CYP79F1*, *CYP79F2*²⁶, and *CYP83A1*⁶³ involved in the core structure formation. The mutants selected here are suitable for studying the role of *BnMYB28* as the ‘master regulator’ of the entire aliphatic GSL biosynthesis process in rapeseed.

We noted that *BnMYB28.A03* single mutants showed a sharper reduction in the seed GSL content compared to the *BnMYB28.C09* single mutants. Furthermore, the seed GSL content in the *BnMYB28* double mutants was at near parity with the *BnMYB28.A03* single mutants. This points to the important role of the *BnMYB28.A03* paralog in GSL metabolism. This is in line with the observation that *BnMYB28.C09* naturally exists in a truncated form in Express617 due to a 4-bp insertion and was found to be associated with reduced seed GSL content⁶⁴. This sheds light on the possibility that in spite of retaining high transcriptional activity and possessing all conserved domains expected for normal protein function, *BnMYB28.C09* is probably non-functional. Therefore, it does not play a critical role in the biosynthesis of GSLs irrespective of the EMS-induced premature stop codon mutation within the first 51 bp of its open reading frame.

Regarding *BnCYP79F1.A06*, only a missense mutation was available where a glutamic acid is replaced by a lysine. Therefore, a weaker phenotypic effect from the *BnCYP79F1* mutations can be explained by a putative compensation effect of *BnCYP79F1.A06*. Since *CYP79F1* can metabolize short and long-chained aliphatic GSLs in *Arabidopsis*²⁶, a possible sub-functionalization in the *B. napus* paralogs could explain the distinct functions of *BnCYP79F1.C05* and *BnCYP79F1.A06*. We speculate that *BnCYP79F1.A06* has a more significant impact on the C5 GSL metabolism than C4 aliphatic GSLs. This is because the sole knock-out of the *BnCYP79F1.C05* paralog in the *BnCYP79F1* double mutants resulted in significant reductions in the short-chained C4 aliphatic GSL progointrin, whereas the C5 glucobrassicinapin content was not significantly reduced. For confirmation, functional analyses of *BnCYP79F1* knock-out mutants for both paralogs are needed.

It is known that the vegetative parts, especially the leaves are a major site for GSL biosynthesis. Although expression of biosynthesis genes is higher in vegetative parts, the seeds show a higher accumulation of GSLs in *Brassica* oilseeds since they are important sink tissues for GSLs in *Brassica* oil crops⁶⁵. Similarly, we observed a significantly higher GSL content in the seeds compared to the leaves. While this observation is in line with previous studies^{9,52,53}, it raises the question as to why GSL levels remain low and mostly unchanged in the leaves even in the mutants. Firstly, since the GSL content was already very low in the leaves, we did not observe any statistically significant reductions in the mutants. Secondly, we reason that the knock-out mutations in biosynthesis genes *BnMYB28* and *BnCYP79F1* described in this study confer restricted aliphatic GSL biosynthesis in the leaves. However, we speculate that a more significant phenotypic effect is realized in the seeds due to the subsequent activity of putative seed-specific GSL transporters^{65,66}.

‘Express’ was a winter type 00-quality rapeseed variety released in 1993. In our study, its derived inbred line Express617 displayed a high seed GSL concentration (49.73 μmol/g DW) which could be due to the following reasons. Firstly, the Express617 line used in this study was developed from Express by repeated selfings (>F₁₁) over the last ~20 years which likely resulted in genetic changes. Also, unintended cross-pollination during the production of inbred lines cannot be fully excluded. Secondly, all experiments were performed under greenhouse

conditions. It is known that GSL content can vary between greenhouse and field grown plants⁶⁷. Moreover, plants were selfed using plastic bags, potentially creating a ‘microclimate’ that could result in increased heat for developing seeds and thereby high seed GSL contents⁶⁸. Nevertheless, the effect of mutations was clearly demonstrated since we compared GSL contents of homozygous mutant and homozygous wild type plants from the same families. Plants homozygous for the wild type allele showed comparable seed GSL contents as non-mutagenized Express617 control plants (Fig. 3). Moreover, our quantitative (GOPOD assay) and qualitative (HPLC) assessment showed corroborative results for total seed GSL content. In the future, the developed double-mutant lines can be grown under field conditions.

In conclusion, our study demonstrates the function of two major genes involved in the biosynthesis of aliphatic GSLs, the most abundant GSL class in rapeseed. Our results provide the first functional analysis by knock-out of *BnMYB28* and *BnCYP79F1* genes in rapeseed. Mutants described in this study displayed significant reductions in the seed aliphatic GSL content that is well within commercial standards. In the future, investigating regulatory shifts in the complex GSL biosynthesis process and the seed-specific transport of GSLs could be crucial for achieving further GSL reduction. Our study provides a strong and promising basis for breeding rapeseed with improved meal quality in the future.

Data availability

The authors declare that data supporting the finding of this study are available from this manuscript and its supplementary information files. Extra data, information, and plant materials used/produced in this study are available from the corresponding author upon request. All local, national or international guidelines and legislation were adhered to in the production of this study.

Received: 11 August 2022; Accepted: 23 January 2023

Published online: 09 February 2023

References

- Russo, M., Yan, F., Stier, A., Klasen, L., & Honermeier, B. Erucic acid concentration of rapeseed (*Brassica napus* L.) oils on the German food retail market. *Food Sci. Nutr.* **9**(7), 3664–3672 (2021).
- Bourdon, D. & Aumaitre, A. Low-glucosinolate rapeseeds and rapeseed meals: Effect of technological treatments on chemical composition, digestible energy content and feeding value for growing pigs. *Anim. Feed Sci. Technol.* **30**(3), 175–191. [https://doi.org/10.1016/0377-8401\(90\)90014-Y](https://doi.org/10.1016/0377-8401(90)90014-Y) (1990).
- Halkier, B. A. & Du, L. The biosynthesis of glucosinolates. *Trends Plant Sci.* **2**(11), 425–431 (1997).
- Sønderby, I. E., Geu-Flores, F. & Halkier, B. A. Biosynthesis of glucosinolates—gene discovery and beyond. *Trends Plant Sci.* **15**(5), 283–290 (2010).
- Blažević, I. *et al.* Glucosinolate structural diversity, identification, chemical synthesis and metabolism in plants. *Phytochemistry* **169**, 112100 (2020).
- Fahy, J. W., Zalcman, A. T. & Talalay, P. The chemical diversity and distribution of glucosinolates and isothiocyanates among plants. *Phytochemistry* **56**(1), 5–51 (2001).
- Mitreiter, S. & Gigolashvili, T. Regulation of glucosinolate biosynthesis. *J. Exp. Bot.* **72**(1), 70–91 (2021).
- Cartea, M. E. & Velasco, P. Glucosinolates in *Brassica* foods: bioavailability in food and significance for human health. *Phytochem. Rev.* **7**(2), 213–229 (2008).
- Velasco, P., Soengas, P., Vilar, M., Cartea, M. E. & del Rio, M. Comparison of glucosinolate profiles in leaf and seed tissues of different *Brassica napus* crops. *J. Am. Soc. Hortic. Sci.* **133**(4), 551–558 (2008).
- Wittkop, B., Snowdon, R. & Friedt, W. Status and perspectives of breeding for enhanced yield and quality of oilseed crops for Europe. *Euphytica* **170**(1), 131–140 (2009).
- Kondra, Z. & Stefansson, B. Inheritance of the major glucosinolates of rapeseed (*Brassica napus*) meal. *Can. J. Plant Sci.* **50**(6), 643–647 (1970).
- Andréasson, E., Jørgensen, L. B., Höglund, A.-S., Rask, L. & Meijer, J. Different myrosinase and idioblast distribution in *Arabidopsis* and *Brassica napus*. *Plant Physiol.* **127**(4), 1750–1763. <https://doi.org/10.1104/pp.010334> (2001).
- Rask, L. *et al.* Myrosinase: gene family evolution and herbivore defense in Brassicaceae. *Plant Mol. Biol.* **42**(1), 93–114 (2000).
- Madlloo, P., Lema, M., Francisco, M., & Soengas, P. Role of Major Glucosinolates in the Defense of Kale Against *Sclerotinia sclerotiorum* and *Xanthomonas campestris* pv. *campestris*. *Phytopathology* **109**(7), 1246–1256 (2019).
- Kaiser, F., Harloff, H. J., Tressel, R. P., Kock, T. & Schulz, C. Effects of highly purified rapeseed protein isolate as fishmeal alternative on nutrient digestibility and growth performance in diets fed to rainbow trout (*Oncorhynchus mykiss*). *Aquac. Nutr.* **27**(5), 1352–1362 (2021).
- Tripathi, M. & Mishra, A. Glucosinolates in animal nutrition: A review. *Anim. Feed Sci. Technol.* **132**(1–2), 1–27 (2007).
- Keck, A.-S. & Finley, J. W. Cruciferous vegetables: cancer protective mechanisms of glucosinolate hydrolysis products and selenium. *Integr. Cancer Ther.* **3**(1), 5–12 (2004).
- Gigolashvili, T., Yatusovich, R., Berger, B., Müller, C. & Flügge, U. I. The R2R3-MYB transcription factor *HAG1/MYB28* is a regulator of methionine-derived glucosinolate biosynthesis in *Arabidopsis thaliana*. *Plant J.* **51**(2), 247–261 (2007).
- Hirai, M. Y. *et al.* Omics-based identification of *Arabidopsis Myb* transcription factors regulating aliphatic glucosinolate biosynthesis. *Proc. Natl. Acad. Sci.* **104**(15), 6478–6483 (2007).
- Yin, L., Chen, H., Cao, B., Lei, J., & Chen, G. Molecular characterization of MYB28 involved in aliphatic glucosinolate biosynthesis in Chinese kale (*Brassica oleracea* var. *alboglabra* Bailey). *Front. Plant Sci.* **8**, 1083 (2017).
- Bisht, N. C. *et al.* Fine mapping of loci involved with glucosinolate biosynthesis in oilseed mustard (*Brassica juncea*) using genomic information from allied species. *Theor. Appl. Genet.* **118**(3), 413–421 (2009).
- Augustine, R., Majee, M., Gershenzon, J. & Bisht, N. C. Four genes encoding MYB28, a major transcriptional regulator of the aliphatic glucosinolate pathway, are differentially expressed in the allopolyploid *Brassica juncea*. *J. Exp. Bot.* **64**(16), 4907–4921. <https://doi.org/10.1093/jxb/ert280> (2013).
- Yang, J. *et al.* Genomic signatures of vegetable and oilseed allopolyploid *Brassica juncea* and genetic loci controlling the accumulation of glucosinolates. *Plant Biotechnol. J.* **19**(12), 2619–2628 (2021).
- Kim, Y. B., Li, X., Kim, S.-J., Kim, H. H., Lee, J., Kim, H., & Park, S. U. MYB transcription factors regulate glucosinolate biosynthesis in different organs of Chinese cabbage (*Brassica rapa* ssp. *pekinensis*). *Molecules* **18**(7), 8682–8695 (2013).
- Reintanz, B. *et al.* *bus*, a bushy *Arabidopsis CYP79F1* knockout mutant with abolished synthesis of short-chain aliphatic glucosinolates. *Plant Cell* **13**(2), 351–367 (2001).

26. Chen, S. *et al.* CYP79F1 and CYP79F2 have distinct functions in the biosynthesis of aliphatic glucosinolates in *Arabidopsis*. *Plant J.* **33**(5), 923–937 (2003).
27. Sharma, M., Mukhopadhyay, A., Gupta, V., Pental, D., & Pradhan, A. K. *BjuB.CYP79F1* regulates synthesis of propyl fraction of aliphatic glucosinolates in oilseed mustard *Brassica juncea*: functional validation through genetic and transgenic approaches. *PLoS One* **11**(2), e0150060 (2016).
28. Li, Z. *et al.* Transcriptome reveals the gene expression patterns of sulforaphane metabolism in broccoli florets. *PLoS ONE* **14**(3), e0213902 (2019).
29. Harper, A. L. *et al.* Associative transcriptomics of traits in the polyploid crop species *Brassica napus*. *Nat. Biotechnol.* **30**(8), 798–802 (2012).
30. Kittipol, V., He, Z., Wang, L., Doheny-Adams, T., Langer, S., & Bancroft, I. Genetic architecture of glucosinolate variation in *Brassica napus*. *J. Plant Physiol.* **240**, 152988. <https://doi.org/10.1016/j.jplph.2019.06.001> (2019).
31. Lu, K. *et al.* Whole-genome resequencing reveals *Brassica napus* origin and genetic loci involved in its improvement. *Nat. Commun.* **10**(1), 1154 (2019).
32. Wei, D. *et al.* Genome-wide identification of loci affecting seed glucosinolate contents in *Brassica napus* L. *J. Integr. Plant Biol.* **61**(5), 611–623. <https://doi.org/10.1111/jipb.12717> (2019).
33. Liu, S. *et al.* Dissection of genetic architecture for glucosinolate accumulations in leaves and seeds of *Brassica napus* by genome-wide association study. *Plant Biotechnol. J.* **18**(6), 1472–1484 (2020).
34. Harloff, H.-J. *et al.* A mutation screening platform for rapeseed (*Brassica napus* L.) and the detection of sinapine biosynthesis mutants. *Theor. Appl. Genet.* **124**(5), 957–969 (2012).
35. Saghai-Marooif, M. A., Soliman, K. M., Jorgensen, R. A. & Allard, R. Ribosomal DNA spacer-length polymorphisms in barley: Mendelian inheritance, chromosomal location, and population dynamics. *Proc. Natl. Acad. Sci.* **81**(24), 8014–8018 (1984).
36. Lee, H. *et al.* Chromosome-scale assembly of winter oilseed rape *Brassica napus*. *Front. Plant Sci.* **11**(496), 1. <https://doi.org/10.3389/fpls.2020.00496> (2020).
37. Till, B. J., Zerr, T., Comai, L. & Henikoff, S. A protocol for TILLING and Ecotilling in plants and animals. *Nat. Protoc.* **1**(5), 2465 (2006).
38. Zerr, T. & Henikoff, S. Automated band mapping in electrophoretic gel images using background information. *Nucleic Acids Res.* **33**(9), 2806–2812 (2005).
39. Fiebig, H. & Arens, M. Glucosinolate (HPLC-Methode) -Gemeinschaftsarbeiten der DGF, 128. Mitteilung: Deutsche Einheitsmethoden zur Untersuchung von Fetten, Fettprodukten, Tensiden und verwandten Stoffen, 98. Mitt.: Analyse von Fettrohstoffen XII*. *12. Fett Wissenschaft Technol.* **94**, 199–203 (1992).
40. Stefanucci, A. *et al.* Chemical characterization, antioxidant properties and enzyme inhibition of Rutabaga root's pulp and peel (*Brassica napus* L.). *Arab. J. Chem.* **13**(9), 7078–7086 (2020).
41. Dubos, C. *et al.* MYB transcription factors in *Arabidopsis*. *Trends Plant Sci.* **15**(10), 573–581 (2010).
42. Guo, Y., Harloff, H.-J., Jung, C. & Molina, C. Mutations in single FT- and TFL1-paralogs of rapeseed (*Brassica napus* L.) and their impact on flowering time and yield components. *Front. Plant Sci.* **5**, 282 (2014).
43. Emrani, N., Harloff, H.-J., Gudi, O., Kopisch-Obuch, F. & Jung, C. Reduction in sinapine content in rapeseed (*Brassica napus* L.) by induced mutations in sinapine biosynthesis genes. *Mol. Breed.* **35**(1), 37. <https://doi.org/10.1007/s11032-015-0236-2> (2015).
44. Braatz, J. *et al.* The effect of INDEHISCENT point mutations on silique shatter resistance in oilseed rape (*Brassica napus*). *Theor. Appl. Genet.* **131**(4), 959–971 (2018).
45. Shah, S., Karunarathna, N. L., Jung, C. & Emrani, N. An APETALA1 ortholog affects plant architecture and seed yield component in oilseed rape (*Brassica napus*). *BMC Plant Biol.* **18**(1), 380. <https://doi.org/10.1186/s12870-018-1606-9> (2018).
46. Sashidhar, N., Harloff, H. J. & Jung, C. Identification of phytic acid mutants in oilseed rape (*Brassica napus*) by large scale screening of mutant populations through amplicon sequencing. *New Phytol.* **225**(5), 2022–2034 (2019).
47. Karunarathna, N. L., Wang, H., Harloff, H. J., Jiang, L. & Jung, C. Elevating seed oil content in a polyploid crop by induced mutations in SEED FATTY ACID REDUCER genes. *Plant Biotechnol. J.* **18**(11), 2251–2266 (2020).
48. Fenwick, G. R. & Curtis, R. F. Rapeseed meal and its use in poultry diets: A review. *Anim. Feed Sci. Technol.* **5**(4), 255–298. [https://doi.org/10.1016/0377-8401\(80\)90016-4](https://doi.org/10.1016/0377-8401(80)90016-4) (1980).
49. Feng, J. *et al.* Characterization of metabolite quantitative trait loci and metabolic networks that control glucosinolate concentration in the seeds and leaves of *Brassica napus*. *New Phytol.* **193**(1), 96–108 (2012).
50. Li, F. *et al.* Genome-wide association study dissects the genetic architecture of seed weight and seed quality in rapeseed (*Brassica napus* L.). *DNA Res.* **21**(4), 355–367 (2014).
51. Toroser, D., Wood, C., Griffiths, H., & Thomas, D. Glucosinolate biosynthesis in oilseed rape (*Brassica napus* L.): studies with 35S³⁵O₂–4 and glucosinolate precursors using oilseed rape pods and seeds. *J. Exp. Bot.* **46**(7), 787–794 (1995).
52. Nour-Eldin, H. H. & Halkier, B. A. Piecing together the transport pathway of aliphatic glucosinolates. *Phytochem. Rev.* **8**(1), 53–67 (2009).
53. Brown, P. D., Tokuhisa, J. G., Reichelt, M. & Gershenzon, J. Variation of glucosinolate accumulation among different organs and developmental stages of *Arabidopsis thaliana*. *Phytochemistry* **62**(3), 471–481 (2003).
54. Howell, P., Sharpe, A. & Lydiat, D. Homoeologous loci control the accumulation of seed glucosinolates in oilseed rape (*Brassica napus*). *Genome* **46**(3), 454–460 (2003).
55. Qu, C.-M. *et al.* Identification of candidate genes for seed glucosinolate content using association mapping in *Brassica napus* L. *Genes* **6**(4), 1215–1229 (2015).
56. Wang, N. *et al.* A functional genomics resource for *Brassica napus*: development of an EMS mutagenized population and discovery of FAE1 point mutations by TILLING. *New Phytol.* **180**(4), 751–765 (2008).
57. Himelblau, E. *et al.* Forward and reverse genetics of rapid-cycling *Brassica oleracea*. *Theor. Appl. Genet.* **118**(5), 953–961 (2009).
58. Stephenson, P. *et al.* A rich TILLING resource for studying gene function in *Brassica rapa*. *BMC Plant Biol.* **10**(1), 62 (2010).
59. Gilchrist, E. J. *et al.* A mutant *Brassica napus* (Canola) population for the identification of new genetic diversity via TILLING and next generation sequencing. *PLoS ONE* **8**(12), e84303 (2013).
60. Tang, S. *et al.* Development and screening of EMS mutants with altered seed oil content or fatty acid composition in *Brassica napus*. *Plant J.* **104**(5), 1410–1422 (2020).
61. Stracke, R., Werber, M. & Weisshaar, B. The R2R3-MYB gene family in *Arabidopsis thaliana*. *Curr. Opin. Plant Biol.* **4**(5), 447–456 (2001).
62. Textor, S., De Kraker, J.-W., Hause, B., Gershenzon, J. & Tokuhisa, J. G. MAM3 catalyzes the formation of all aliphatic glucosinolate chain lengths in *Arabidopsis*. *Plant Physiol.* **144**(1), 60–71 (2007).
63. Hamm, M. R., Ruegger, M. O. & Chapple, C. The *Arabidopsis ref2* mutant is defective in the gene encoding CYP83A1 and shows both phenylpropanoid and glucosinolate phenotypes. *Plant Cell* **15**(1), 179–194. <https://doi.org/10.1105/tpc.006544> (2003).
64. Schilbert, H. M. *et al.* Mapping-by-sequencing reveals genomic regions associated with seed quality parameters in *Brassica napus*. *Genes (Basel)* **13**(7), 1. <https://doi.org/10.3390/genes13071131> (2022).
65. Nour-Eldin, H. H. *et al.* Reduction of antinutritional glucosinolates in *Brassica* oilseeds by mutation of genes encoding transporters. *Nat. Biotechnol.* **35**, 377 (2017).
66. Nambiar, D. M. *et al.* GTR1 and GTR2 transporters differentially regulate tissue-specific glucosinolate contents and defence responses in the oilseed crop *Brassica juncea*. *Plant Cell Environ.* **44**(8), 2729–2743 (2021).

67. Kim, K. H. & Chung, S.-O. Comparison of plant growth and Glucosinolates of Chinese cabbage and Kale crops under three cultivation conditions. *J. Biosyst. Eng.* **43**(1), 30–36 (2018).
68. Justen, V. L. & Fritz, V. A. Temperature-induced glucosinolate accumulation is associated with expression of BrMYB transcription factors. *HortScience* **48**(1), 47–52 (2013).

Acknowledgements

We thank Monika Bruisch and Brigitte Neidhardt-Olf for their assistance in greenhouse experiments. We acknowledge the support provided by Jens Hermann and Prof. Dr. Wolfgang Bilger from the Department of Ecophysiology of Plants in Kiel for HPLC analytics. We also thank the Institute of Clinical Molecular Biology in Kiel for providing Sanger sequencing services. This work was financially supported by the Federal Ministry of Education and Research (BMBF) within the project IRFFA: Improved Rapeseed as Fish Feed in Aquaculture (grant number 031B0357B).

Author contributions

S.J., H.J.H. and C.J. designed the research. S.J. conducted the experiments and analyzed the data. C.W., M.B. and D.T. provided support for the qualitative assessment of glucosinolates. H.J.H. and C.J. supervised the research. S.J. wrote the original draft. H.J.H., A.A., M.B., C.W., D.T. and C.J. reviewed and edited the manuscript. All authors participated in the discussion and revision of the manuscript. The authors read and approved the final manuscript.

Funding

Open Access funding enabled and organized by Projekt DEAL. This work was funded by the Federal Ministry of Education and Research (BMBF) within the framework of the project IRFFA: Improved Rapeseed as Fish Feed in Aquaculture (grant number 031B0357B).

Competing interests

AA is employed by NPZ Innovation GmbH, Germany. The remaining authors declare that the research was conducted in the absence of any commercial or financial relationships and declare no competing interests.

Additional information

Supplementary Information The online version contains supplementary material available at <https://doi.org/10.1038/s41598-023-28661-6>.

Correspondence and requests for materials should be addressed to C.J.

Reprints and permissions information is available at www.nature.com/reprints.

Publisher's note Springer Nature remains neutral with regard to jurisdictional claims in published maps and institutional affiliations.



Open Access This article is licensed under a Creative Commons Attribution 4.0 International License, which permits use, sharing, adaptation, distribution and reproduction in any medium or format, as long as you give appropriate credit to the original author(s) and the source, provide a link to the Creative Commons licence, and indicate if changes were made. The images or other third party material in this article are included in the article's Creative Commons licence, unless indicated otherwise in a credit line to the material. If material is not included in the article's Creative Commons licence and your intended use is not permitted by statutory regulation or exceeds the permitted use, you will need to obtain permission directly from the copyright holder. To view a copy of this licence, visit <http://creativecommons.org/licenses/by/4.0/>.

© The Author(s) 2023